Cerebral Cortex, December 2017;27: 5683–5695

doi: 10.1093/cercor/bhw339
Advance Access Publication Date: 2 December 2016
Original Article

ORIGINAL ARTICLE

Migration Pathways of Thalamic Neurons and Development of Thalamocortical Connections in Humans Revealed by Diffusion MR Tractography

Molly Wilkinson[1], Tara Kane [1,2], Rongpin Wang[2,3] and Emi Takahashi[2,4]

[1]Department of Behavioral Neuroscience, Northeastern University, Boston, MA 02115, USA, [2]Division of Newborn Medicine, Department of Medicine, Boston Children's Hospital, Harvard Medical School, 300 Longwood Avenue, Boston, MA 02115, USA, [3]Department of Radiology, Guizhou Provincial People's Hospital, 83 Zhong Shan Dong Lu, Guiyang, Guizhou Province 550002, P.R. China and [4]Athinoula A. Martinos Center for Biomedical Imaging, Massachusetts General Hospital, Harvard Medical School, Charlestown, MA 02219, USA

Address correspondence to Emi Takahashi, Division of Newborn Medicine, Department of Medicine, Boston Children's Hospital, Harvard Medical School, 1 Autumn St. #456, Boston, MA 02115, USA. Email: emi@nmr.mgh.harvard.edu.

Abstract

The thalamus plays an important role in signal relays in the brain, with thalamocortical (TC) neuronal pathways linked to various sensory/cognitive functions. In this study, we aimed to see fetal and postnatal development of the thalamus including neuronal migration to the thalamus and the emergence/maturation of the TC pathways. Pathways from/to the thalami of human postmortem fetuses and in vivo subjects ranging from newborns to adults with no neurological histories were studied using high angular resolution diffusion MR imaging (HARDI) tractography. Pathways likely linked to neuronal migration from the ventricular zone and ganglionic eminence (GE) to the thalami were both successfully detected. Between the ventricular zone and thalami, more tractography pathways were found in anterior compared with posterior regions, which was well in agreement with postnatal observations that the anterior TC segment had more tract count and volume than the posterior segment. Three different pathways likely linked to neuronal migration from the GE to the thalami were detected. No hemispheric asymmetry of the TC pathways was quantitatively observed during development. These results suggest that HARDI tractography is useful to identify multiple differential neuronal migration pathways in human brains, and regional differences in brain development in fetal ages persisted in postnatal development.

Key words: brain, development, diffusion imaging, human, neuronal migration, thalamocortical, tractography, white matter

Introduction

The thalamocortical (TC) axonal pathways serve as a basis for a variety of important brain functions such as sensory relay (Jones 2007), consciousness (Llinás 2003), working memory (Sarnthein et al. 2005), executive control, and salience processing (Seeley et al. 2007), by facilitating communication between neurons in the thalamus and neurons throughout the cortex. The TC system is already active early in prenatal embryonic life (Catalano and Shatz 1998; Molnár et al. 2003). Alcauter et al. (2014) found that human neonatal brains, around 33 days old, had already developed the thalamus–sensorimotor and thalamus–salience networks that are important in later life.

Neuronal migration is an essential part of brain development, allowing neurons to find and settle in their terminal positions to effectively interact with each other (Sidman and Rakic 1973). Without successful thalamic neuronal migration, developmental disorders can occur, such as schizophrenia (Jones 1997) and dyslexia (Galaburda 2005). The thalamic

neurons follow nonradial migration, as well as radial migration routes (Frassoni et al. 2000). Excitatory glutamatergic projection neurons and a portion of GABAergic neurons originate in the proliferative dorsopallial ventricular/subventricular zone and migrate along radial glial fascicles to the cortical plate (Rakic 1972, 1988; Bystron et al. 2008; Petanjek et al 2009a, 2009b). The other major migratory routes are mainly in the ganglionic eminence (GE); they run tangential to the cortical plate and contain inhibitory GABAergic interneurons (Frassoni et al. 2000; Ortino et al. 2003; Wonders and Anderson 2006). Both migration pathways have been clearly imaged in our studies as coherent fiber pathways (Takahashi et al. 2012; Kolasinski et al. 2013; Miyazaki et al. 2016); however, the development of the thalamus and TC pathways was not analyzed in any of these studies.

Rakić and Sidman (1969; see also review article by Sidman and Rakić 1973) showed that during the early gestational weeks (GW) (around 10 GW) of human development, the ventricular zone of the third ventricle contributes to supplying neurons to the thalamus, and in later stages (around 24 GW) neuronal migration was observed from the GE and the corpus gangliothalamicum in the telencephalon. Since macaque monkeys do not receive neurons from the telencephalon, they speculated that such nonradial neuronal migration may be contributing to the unique capacities of humans, followed by direct evidence to prove that concept (Letinić and Rakić 2001; see also review of Rao and Wu 2001; Corbin et al. 2001). The ventral telencephalon was shown to be the place of origin of the cells that will eventually migrate to the thalamus through the nonradial route (Rakić and Sidman 1969; Letinić and Kostović 1997; Corbin et al. 2001).

Neurons begin migration from the ventricular zone toward the pia mater around embryonic day (E) 31–32 (Bystron et al. 2008). Globally, the most migratory activity also occurs around GW12–20, and a distinct pathway likely related to migration was detected from the GE to the dorsal thalamus from GW15–26 (Letinić and Rakić 2001). Between GW11 and GW13, thalamic pulvinar fibers extend to the temporoparieto-occipital confluence, but they begin to enter the occipital lobe in large numbers around GW17–20 and have formed a well-defined thalamic radiation by GW25 (Kostovic and Rakic 1984). It was found that radial migration is almost complete at GW26 as radial glia are replaced by astrocytes and thalamic afferent fibers develop, but it is still found to be intact in certain regions like the occipital lobe at GW30 (Xu et al. 2014). By 36 weeks, the radial glia have almost completely disappeared and TC afferent fibers have finished forming (McKinstry et al. 2002). The nonradial migration pathway is also found to be thickest at GW17, increasingly sparse at GW30, and unidentifiable at GW34 (Miyazaki et al 2016).

Many previous tractography studies have been done on the TC pathways in adults (e.g., Johansen-Berg et al. 2005; Yamada et al. 2007; Jaermann et al. 2008; Hong et al. 2010; Klein et al. 2010; Zhang et al. 2010). A diffusion tensor imaging (DTI) tractography study on the Papez circuit, in 26 healthy adults between 21 and 77 years old (Jang and Yeo 2013), reconstructed the TC tracts from the anterior thalamic nuclei, through the genu of the internal capsule, the anterior limb of the internal capsule, and the white matter around the anterior horn of the lateral ventricle and ending in the anterior cingulate gyrus. This study found no significant differences between hemispheres of some diffusion indices and tract volume in the Papez circuit.

High angular resolution diffusion MR imaging (HARDI) tractography enables identification of complex crossing tissue coherence in the brain (Tuch 2004) even in immature fetal brains (Takahashi et al. 2012, 2014), which are typically more challenging to segment due to a surplus of unmyelinated fibers. HARDI tractography allows reconstruction of water diffusivity in many different directions in each imaging voxel. Using a high-field MRI scanner allows us to see "very high-resolution" water diffusion from which we can infer neuronal pathways; however, it does not directly show specific axons or glial fibers (Takahashi et al. 2012). Still, this technique theoretically provides an advantage over DTI (Mori and van Zijl 2002; Frank 2002; Tournier et al. 2004), because there are many places throughout the brain where the white matter tracts cross, going in many different directions (Tournier et al. 2007). Our previous studies (Takahashi et al. 2012; Kolasinski et al. 2013; Miyazaki et al. 2016) successfully showed overall courses of radial and nonradial neuronal migration pathways using diffusion tractography. However, those studies did not specifically describe pathways related to the thalamus. In this study, we aimed to image and qualitatively describe neuronal migration pathways related to the thalamus and pathways likely corresponding to thalamic axons in the human fetal brain, and to quantify the development of the TC pathways from newborn to adult ages.

After birth, the human brain significantly grows during the first few years of life (Thompson 2001; Lippé et al. 2009; Gredebäck and Kochukhova 2010; Berchicci et al. 2011), and there have been a considerable number of findings and discussions that suggest children around 3 years old already have a brain very close to the size of an adult brain, with matured white and gray matter MRI contrast and diffusion properties of tracts, as well as matured cognitive patterns that can be a basis for adult cognitive functions (Schimdt and Beauchamp 1988; Berthier et al. 2000; Whiten et al. 2006; Keen and Shutts 2007; Keitel et al. 2013; Smith et al. 2015). Given these findings, in one way to study brain development, one can assume the group of 3 years and younger to be "before or during the first significant brain growth in life" and the group of older than 3 years to be "after the first significant brain growth in life." Therefore, for postnatal analyses, we focused on the difference between the 2 groups in this study: 3 years and younger, and older than 3 years (Cohen et al. 2016).

Materials and Methods

Postmortem Fetal Brain Specimens

Eleven postmortem fetal brains' data were used in this study. Eight postmortem brains (one 17 GW, two 18 GW, three 20 GW, one 31 GW, and one postnatal 20 months old) were obtained from the Department of Pathology, Brigham and Women's Hospital (Boston, MA, USA), and 3 postmortem brains (19, 21, and 22 GW) were provided by the Allen Institute Brain Bank (Seattle, WA, USA). Postmortem specimens were obtained with full parental consent. The brains were grossly normal, and standard autopsy examination of all brains revealed minimal or no pathologic abnormalities at the macroscopic level.

In Vivo Subjects

Initially, we selected 90 subjects with our inclusion criteria (no neurological/psychiatric history and no MRI-based abnormalities). Newborns and infants were scanned during sleep, mostly with sedation but some without. Seven subjects were excluded based on motion artifacts (4 newborns/infants younger than 1 year, one 3-year-old, one 6-year-old, and one 9-year-old subjects). The remaining 83 subjects from newborn to 28 years old

had clinically indicated brain MRI studies that were interpreted to show no abnormalities. None had clinical concerns for a congenital malformation or genetic disorder. All research protocols were approved by the institutional review board.

Tissue Preparation for HARDI

At the time of autopsy, all brains were immersion fixed, the brains from the Brigham and Women's Hospital were stored in 4% paraformaldehyde, and the brains from the Allen Institute Brain Bank were stored in 4% periodate-lysine-paraformaldehyde (PLP). During MR imaging acquisition, the brains from the Brigham and Women's Hospital were placed in Fomblin solution (Ausimont, Thorofare, NJ, USA) (Takahashi et al. 2012) and the brains from the Allen Institute Brain Bank were placed in 4% PLP. These different kinds of solutions in which the brains from different institutes were placed tend to change the background contrast (i.e., we see dark background outside of the brain using Fomblin and bright background using PLP), but they do not specifically change diffusion properties (e.g., fractional anisotropy [FA] and apparent diffusion coefficient [ADC]) within the brain.

Diffusion MRI Procedures

The postmortem brain specimens from the Brigham and Women's Hospital were imaged at a 4.7 T Bruker Biospec MR system (specimens from 17 to 31 GW) and specimens from the Allen Institute Brain Bank were imaged at a 3 T Siemens MR system (3 fetal [19, 20, 22 GW] specimens) at A. A. Martinos Center, Massachusetts General Hospital, Boston, MA, USA. The reason why we used the 3 T system was that the brains from the Brain Bank were "in cranio" and did not fit in the 4.7 T bore. To improve the imaging quality and obtain the best signal to noise and high spatial resolution, however, we used a custom-made MR coil at the 3 T system that just fit the specimens. Different scanner systems were used to accommodate the different brain sizes, and MR coils that best fit each brain sample were used to ensure optimal imaging.

A 3-dimensional (3D) diffusion-weighted spin-echo echo-planar imaging (SE-EPI) sequence was used with a repetition time/echo time (TR/TE) 1000/40 ms, with an imaging matrix of 112 × 112 × 112 pixels. Sixty diffusion-weighted measurements (with the strength of the diffusion weighting, $b = 8000\ s/mm^2$) and 1 non–diffusion-weighted measurement (no diffusion weighting or $b = 0\ s/mm^2$) were acquired with the duration of the diffusion gradients, $\delta = 12.0$ ms, and the time interval between the start of the 2 diffusion gradients, $\Delta = 24.2$ ms. The total acquisition time was approximately 2 h for each imaging session. The spatial resolution was 400 × 500 × 500 μm for brains from 17 to 22 GW and 520 × 520 × 600 μm for 30–31 GW. We determined the highest spatial resolution for each brain specimen with an acceptable signal-to-noise ratio of more than 130 and within a reasonable scan time of 2 h.

For the living healthy subjects, T_1-weighted MPRAGE imaging, T_2-weighted turbo spin-echo imaging, and a diffusion-weighted SE-EPI were performed. Thirty diffusion-weighted measurements ($b = 1000\ s/mm^2$) and 5 non–diffusion-weighted measurements ($b = 0\ s/mm^2$) were acquired on a 3 T MR system (Skyra, Siemens Medical Systems) with TR = 10 s, TE = 88 ms, $\delta = 12.0$ ms, $\Delta = 24.2$ ms, field of view = 22 × 22 cm, spatial resolution 2 × 2 × 2 mm, matrix size = 128 × 128, and iPAT = 2.

Diffusion Data Reconstruction for Tractography

DiffusionToolkit and TrackVis (trackvis.org) were used to reconstruct and visualize tractography pathways. Tractography pathways were reconstructed using a HARDI model with a streamline/FACT algorithm and a 45° angle threshold. No threshold of FA was used for the fiber reconstruction. Brain mask volumes were used to terminate tractography structures instead of the standard FA threshold (Takahashi et al. 2010, 2011, 2012, 2014; Schmahmann et al. 2007; Wedeen et al. 2008; Song et al. 2015), because progressive myelination and crossing fibers in the developing brain can result in low FA values that may potentially incorrectly terminate tractography tracing in brain regions with low FA values.

Tract Delineation

To delineate pathways connecting with the thalami, which may include both neuronal migration pathways to the thalami and TC pathways, regions of interest (ROIs) were placed using DTI and tractography atlases (Wakana et al., 2004; Mori and van Zijl, 2007; Catani and Thiebaut de Schotten, 2008), in the thalami, cerebral cortex, and internal capsule regions. The ROIs were carefully optimized not to include other white matter pathways as well as not to miss the TC pathways by changing the size and location several times. We also occasionally used additional ROIs to exclude clearly different pathways from the pathways of interest.

For each subject, a "whole-brain" (WB) tract group was created (used for normalizing results; see below), which was identified as the sum of all streamlines identified within the entire intracranial brain space.

The color coding of tractography pathways in Figures 1, 2, and 4 was based on a standard red–green–blue (RGB) code that was applied to the vector in each brain area to show the spatial locations of terminal regions of each pathway (red for right–left, green for dorsal–ventral, and blue for anterior–posterior). In Figure 3, pathways from/to the thalamus in panels A–C and pathways related to the GE in panel D were color coded in a single color (yellow). The other pathways in Figure 3 were color coded as in Figures 1, 2, and 4.

Quantification

FA, ADC, tract number, length, and volume were measured on reconstructed tractography in each subject, using TrackVis.

Raw data of each type of measurement were further normalized using 2 schemes: an "18Y+" normalization and a "WB" normalization. In the 18Y+ normalization, individual subjects' data were compared with the average value in all subjects 18 years or older, separately in the left and right hemispheres. The intent of this normalization was to compare an individual's tracts to those of a mature adult. In the WB normalization, we combined left and right hemispheric data into a single mean value, and each individual's quantities were divided by that of the sum of all intracranially identified brain pathways in the same individual (i.e., the WB tract group described above). The intent of this normalization was to account for individual variations in brain volume and tract characteristics.

Left and right hemispheric data (L and R) for each pathway were used to calculate laterality index (LI). LIs were calculated as follows: $LI = (L - R)/[0.5 \times (L + R)]$. LIs range from −2 to 2, and positive and negative LI values correspond to left and rightward asymmetry, respectively (Caviness et al. 1996; Thiebaut de Schotten et al. 2011; Song et al. 2015).

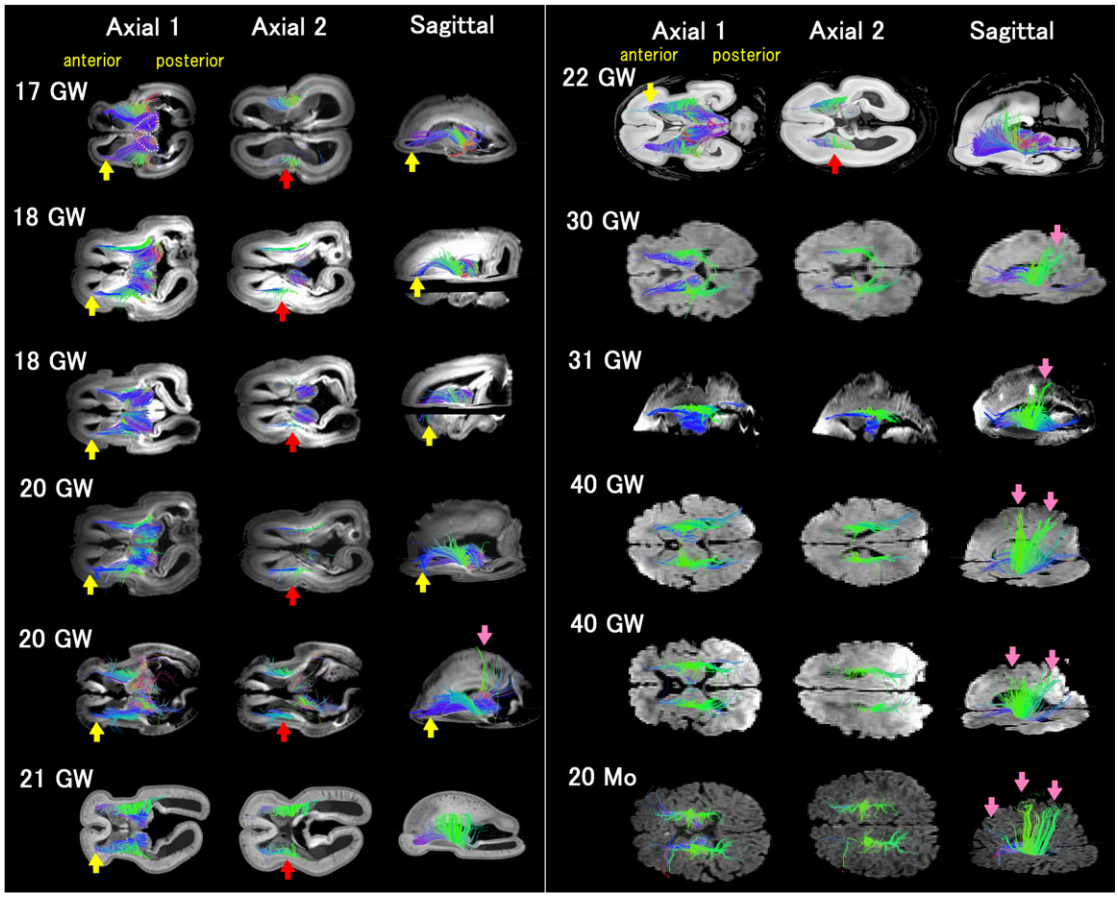

Figure 1. Representative tractography pathways identified as streamlines running from/to the thalami from 17 GW to postnatal 20 months old (Mo). The same tractography pathways identified within a brain from/to the thalami are shown in 2 axial views and 1 sagittal view using anatomical reference images (mean diffusion-weighted images in a gray scale). The grayscale image in Axial 1 shows the level of a middle part of the thalamus, while another grayscale image in Axial 2 shows a more dorsal slice, close to a level of the upper edge of the thalami. The sagittal images are set around the mesial aspect of one of the hemispheres. Note that only the right hemisphere was available for 31 GW in this study. The color coding of tractography pathways is based on a standard RGB code that is applied to the vector in each brain area to show the spatial locations of terminal regions of each pathway (red for right–left, green for dorsal–ventral, and blue for anterior–posterior). Yellow arrows indicate the edge of anterior ventricle regions where tractography pathways were connected. Such pathways were running tangentially along the edge of the ventricle and projected to the thalami (e.g., white dotted lines in 17 GW). Red arrows indicate that the middle part of the identified tractography pathways penetrated into deep white matter regions. Pink arrows indicate pathways projected into the cortical gray matter.

Statistical Analysis

Subject data were divided into 2 groups: 3 years and younger (24 subjects) and older than 3 years (59 subjects). Statistical significance was set to $P < 6.7 \times 10^{-4}$ ($P < 0.01/15$ [Bonferroni correction for multiple comparisons with 5 measurements {tract count, volume, length, FA, and ADC} × either 3 TC segments {anterior, middle, and posterior} or the comparisons among the 3 segments {anterior to middle, middle to posterior, and anterior to posterior}]). The laterality tests were done by comparing LIs to zero. Statistical significance was set to $P < 0.01$ for the laterality test.

Results

Descriptive Analyses: Ex Vivo and In Vivo Data

Pathways Identified by Thalamus ROIs

Both ex vivo and in vivo data were used for all the descriptive analyses. Tractography pathways originating from the ROIs for the thalami were detected in all studied brains (Fig. 1). The leftmost column (Axial 1) for each subject shows axial slices that pass the center of the thalami, the middle column (Axial 2) shows axial slices of the upper part of the brain, at the top part of the brain (around the primary sensory/motor areas). The rightmost column (Sagittal) for each subject shows an oblique sagittal view. From 17 to 22 GW, tractography pathways in anterior and posterior regions were connected with the edge of the ventricle (yellow arrows in Fig. 1 for anterior regions and example magnified images in Fig. 2A). Such pathways were running tangentially along the edge of the ventricle and projected to the thalami (e.g., white dotted lines in 17 GW in Figs 1 and 2A).

While the anterior and posterior sections of the pathways related to the thalami clearly originated only from the edge of the ventricle in early gestational ages (17–22 GW), the middle section of the pathways mostly went up into the deep regions in the cerebral mantle (red arrows in Figs 1 and 2A). It was clear that the middle section of the tractography pathways penetrating into the cortex was imaged starting from 30 GW (pink arrow in Figs 1 and 2B), except for one of the 20 GW samples.

At 17 GW, many pathways connecting with the ventricle were clearly imaged in the anterior part of the brain (Fig. 2A, yellow arrow), some existed in the middle part of the brain (Fig. 2A), and a much smaller number of pathways were found

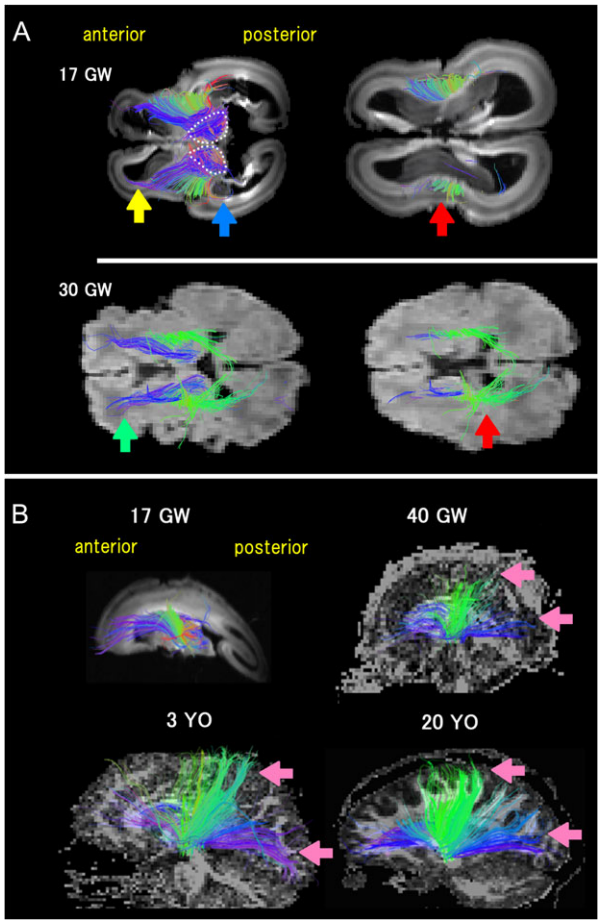

Figure 2. (*A*) Magnified images of axial views of 17 and 30 GW from Figure 1. Yellow and blue arrows indicate the edge of anterior (yellow) and posterior (blue) ventricle regions where tractography pathways from/to the thalami were connected. Green arrow at 30 GW indicates white matter pathways running in a similar course with that taken by the pathways indicated by yellow arrow at 17 GW, but do not connect to the edge of the ventricle. White dotted lines at 17 GW outline the edge of the thalami. Red arrows indicate that the middle part of the identified tractography pathways penetrated into deep white matter regions. (*B*) Sagittal views of 17 GW, 40 GW, 3 years old (YO), and 20 YO. Pink arrows indicate pathways projected into the cortical gray matter. The color coding of tractography pathways is the same as used in Figure 1.

in the posterior part (Fig. 2*A*, blue arrow). This tendency continued through 22 GW (Fig. 1), with gradual decrease in the number of the pathways in the anterior region. It was noticed that the pathways to the anterior region are identified as several bundles of axons (e.g., Fig. 2*B*, 17 GW), although not in all specimens. At 30 GW, there were no pathways observed from the edge of the ventricle (Fig. 2*A*). There were pathways detected running in the similar courses to the GE-related pathways, but those pathways were off from the ventricle, running through white matter regions (green arrow in Fig. 2*A*). The same tendency was found in late gestational ages (31 GW, 40 GW, and older).

Spatial Relationships Between Pathways Identified by Thalamus and GE ROIs

Pathways described above between the thalami and the ventricular zone took a course just below the main body of the GE, the structure with blue/purple pathways in Figure 3*A–C* (in yellow in Fig. 3*D* for a visualization purpose). While the anterior portion of the GE pathways and pathways from/to the thalamus were found to be running along each other (Fig. 3*A*), the middle and posterior regions showed distinct trajectories of the 2 pathways: the main body of the GE showed strong coherency in the anterior–posterior direction (Fig. 3*B* and *C*), while pathways related to the thalamus were running toward the surface of the brain in the middle part (red arrows in Fig. 3*B* and *C*). The posterior thalamic-related pathways were found at the edge of the ventricle running tangentially to the ventricle, while the GE pathways were found running dorso-ventrally, perpendicular to the thalamic-related pathways (Fig. 3*B*). Such trends were observed until 21 GW (Fig. 3*D*).

Pathways Identified by GE ROIs

By carefully moving ROIs along the GE structure, 3 distinct pathways between the GE and the thalami were identified: 1) a part of the anterior GE was connected to middle regions of the thalami (Fig. 4*A*, yellow arrows), 2) a part of the dorsal GE was connected to dorsal superficial regions of the thalami (Fig. 4*B*, red arrows), and 3) the mid-posterior GE was connected to posterior and middle parts of the thalami, anatomically corresponding to the ventral complex (Bayer and Altman 2005) (Fig. 4*C*, green arrows).

Quantitative Analyses: In Vivo Data From Newborn to Adult Ages

Difference Among Anterior, Middle, and Posterior Segments

All measures were obtained and compared across the anterior, middle, and posterior segments (Table 1). The middle segment had significantly more tract count and volume than those of the anterior and posterior segments, and the anterior segment had significantly more tract count and volume than those of the posterior segment (posterior < anterior < middle). The length of the middle segment was longer than the length of the anterior segment, while the length of the posterior segment was longer than the length of the anterior or middle segment (anterior < middle < posterior). FA and ADC values did not show any difference in studied comparisons except for FA values between the anterior and posterior segments (anterior < posterior). Scatter plots for all measures can be found in Supplementary Figures S1 (for left and right sides separately) and S2 (left and right sides averaged).

Normalized Data Using Mean Adult Values (18+ Normalization)

Next, we compared measured properties of each segment of the pathways between the group of 3 years and younger, and the older than 3 years group (Table 2). Normalized data using mean adult values (18+ normalization) showed standard developmental patterns: increased tract count, volume, and length. FA and ADC values did not show significant differences, although the comparisons in FA and ADC values in anterior and posterior segments were significant if using a lenient threshold of *P* values ($P = 0.01$) without a correction for multiple comparisons. Scatter plots for all measures can be found in Supplementary Figure S3.

WB Normalization

Next, we calculated normalized values using each subject's WB pathways and compared WB-normalized measured properties of each segment of the pathways between the group of 3 years and younger, and the group older than 3 years (Table 3). Anterior TC pathways in the group of 3 years and younger had

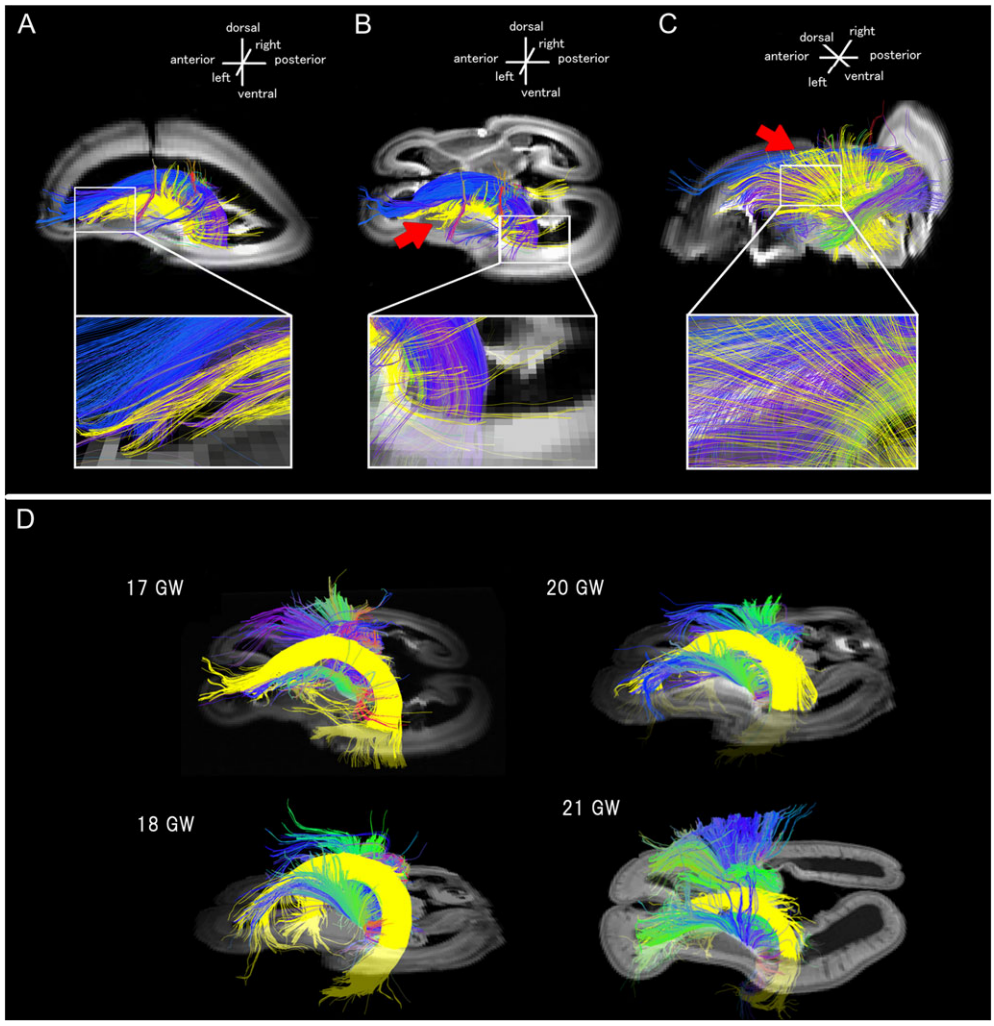

Figure 3. A) Oblique sagittal and (*B*) oblique axial views, and (*C*) an oblique view from the bottom of the brain of a 17 GW brain, and (*D*) oblique axial views of brains at 17 GW, 18 GW, 20 GW, and 21 GW. In (*A–C*), the pathways from/to the thalamus are shown in yellow and pathways linked to the GE are color coded based on the standard RGB code that is used in Figure 1. Red arrows indicate pathways from/to the thalamus running perpendicularly to the GE pathways, toward the surface of the brain. In (*D*), the GE-linked pathways are shown in yellow and pathways from/to the thalami are color coded based on the standard RGB code used in Figure 1.

more WB-normalized tract number and volume than older than 3 years, respectively. Middle and posterior segments of the TC pathways did not show difference in tract number nor in volume before and after 3 years old. WB-normalized length was longer in older groups in the posterior segment, while the anterior and middle segments showed no significant difference. WB-normalized FA values increased after 3 years old in all segments. ADC values did not show significant differences; however, they were significant with a more lenient threshold without a correction for multiple comparisons (0.01 or 0.05). Scatter plots for all measures can be found in Supplementary Figure S4.

Laterality

There was no overall significant laterality in any of the 3 segments in any studied measurements ($P > 0.05$). We confirmed with other different age groupings (at or before 1.5, 5, or 10 years old vs. after 1.5, 5, or 10 years old) that none of the groupings showed significant laterality ($P > 0.05$).

Discussion

Pathways from/to the thalami of human postmortem fetuses and in vivo subjects ranging from newborns to adults with no neurological histories were studied using HARDI tractography. Pathways likely linked to neuronal migration from the ventricular zone and the GE to the thalami were both successfully detected in a 3D manner. Between the ventricular zone and thalami, more tractography pathways were found in the anterior regions compared with posterior regions, which was in well agreement with postnatal observations that the anterior TC segment had more tract count and volume than the posterior TC segment. No hemispheric asymmetry of the TC pathways was quantitatively observed during development. Regarding the GE pathways, 3 differential pathways likely linked to neuronal migration from the GE to the thalami were detected between the anterior GE to the middle part of the thalami, between the dorsal GE to the dorsal thalami, and between the mid-posterior GE to the mid-posterior thalami. These results suggest that HARDI tractography is useful to identify multiple differential neuronal migration pathways in human brains.

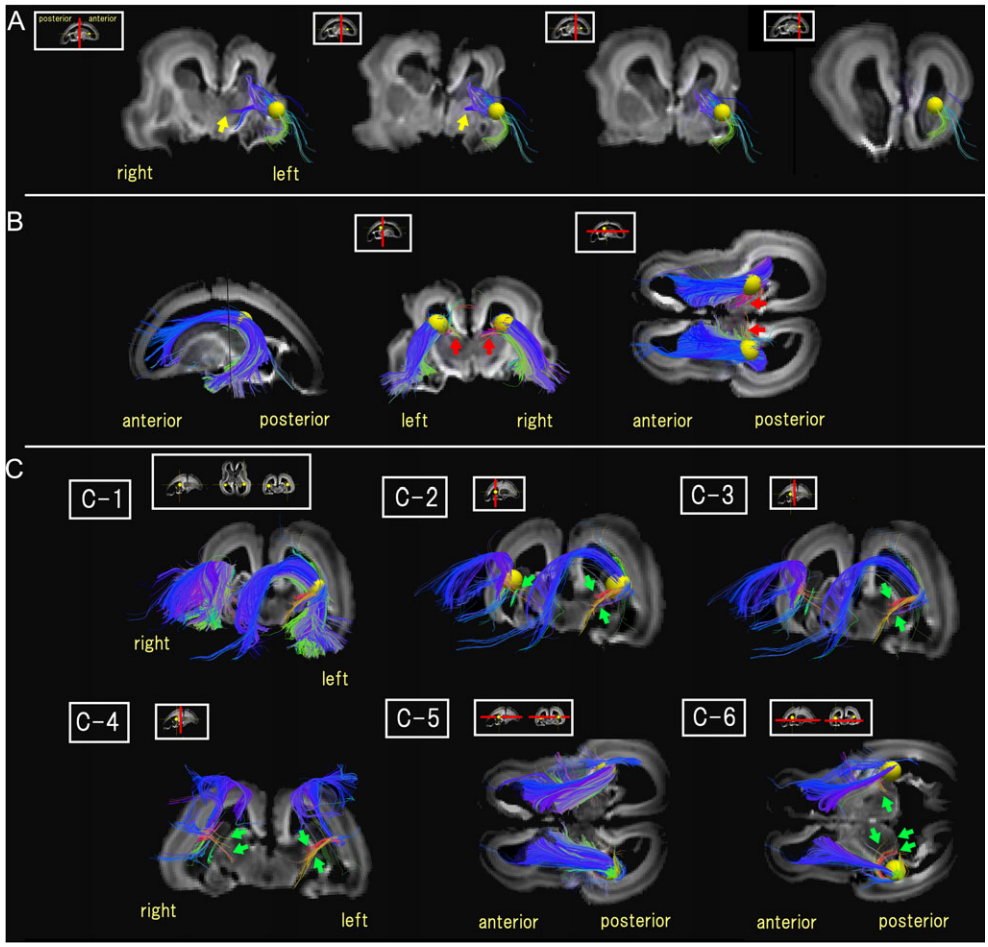

Figure 4. Three distinct pathways between the GE and the thalami detected by diffusion tractography. (*A*) Pathways running through the yellow sphere placed in an anterior GE region. Sequential oblique coronal views from the left, at the level of the thalamus to more anterior brain regions are shown. The anterior GE region connected to middle regions of the thalami (yellow arrows). Some pathways look like running outside of the brain, but this is due to the oblique angle of the coronal images and 3D fiber trajectories. (*B*) Pathways running through the yellow sphere placed in a dorsal GE region. Sagittal (left), coronal (middle), and axial (right) views are shown. The dorsal GE region was connected to dorsal superficial regions of the thalami (red arrows). (*C*) Pathways running through the yellow sphere placed in a mid-posterior GE region. (*C-1–C-3*) Oblique coronal views from the left, (*C-4*) an oblique coronal view from the bottom, and (*C-5*, *C-6*) axial views. (*C-1*, *C-5*) All pathways detected using the yellow sphere (all pathways running through and from/to the sphere). (*C-2–C-4*, *C-6*) Pathways only from/to the yellow sphere for a visualization purpose. The mid-posterior GE region was connected to posterior and middle parts of the thalami, anatomically corresponding to the ventral complex (green arrows). A small insert in the upper left corner of each panel shows the level of the image slice as a red line. The color coding of tractography pathways is the same as used in Figure 1.

Table 1 Mean and standard deviation (raw data: all ages, under 3 YO, and over 3 YO) of each segment, and 3 segments comparison (all ages)

		Tract count	Volume (mL)	Length (mm)	FA	ADC (mm^2/s for mean ± SD)
Anterior: mean ± SD	All ages	275.2 ± 76.9	1258.4 ± 338.7	27.4 ± 4.4	0.45 ± 0.06	7.61 ± 0.79
	Under 3 YO	192.5 ± 52.5	831.9 ± 198.0	22.7 ± 3.7	0.40 ± 0.08	7.94 ± 0.14
	Over 3 YO	305.6 ± 72.0	1416.1 ± 305.0	29.0 ± 4.2	0.47 ± 0.04	7.49 ± 0.60
Middle: mean ± SD	All ages	674.0 ± 234.8	2675.5 ± 848.0	48.4 ± 5.7	0.48 ± 0.05	7.53 ± 0.88
	Under 3 YO	385.4 ± 95.3	1466.7 ± 331.5	41.3 ± 4.4	0.47 ± 0.10	7.90 ± 0.16
	Over 3 YO	780.7 ± 193.3	3121.5 ± 572.1	51.0 ± 4.3	0.49 ± 0.03	7.41 ± 0.70
Posterior: mean ± SD	All ages	151.9 ± 53.3	932.3 ± 288.1	56.6 ± 8.1	0.52 ± 0.06	8.00 ± 0.92
	Under 3 YO	89.8 ± 39.7	544.5 ± 189.1	47.5 ± 8.2	0.46 ± 0.08	8.37 ± 0.17
	Over 3 YO	174.0 ± 45.6	1074.9 ± 214.8	60.0 ± 6.3	0.54 ± 0.04	7.86 ± 0.72
Anterior to middle	*P* values (anterior vs. middle)	**1.44×10^{-23}**	**1.79×10^{-21}**	**6.64×10^{-46}**	5.01×10^{-3}	6.71×10^{-1}
	Bigger mean value	Middle	Middle	Middle		
Middle to posterior	*P* values (middle vs. posterior)	**4.64×10^{-35}**	**1.11×10^{-29}**	**1.94×10^{-8}**	2.71×10^{-3}	2.54×10^{-2}
	Bigger mean value	Middle	Middle	Posterior		
Anterior to posterior	*P* values (anterior vs. posterior)	**1.91×10^{-15}**	**5.70×10^{-7}**	**2.20×10^{-50}**	**8.31×10^{-8}**	4.82×10^{-2}
	Bigger mean value	Anterior	Anterior	Posterior	Posterior	

*Statistically significant *P* values are bolded.

Table 2 *P* values, mean, and standard deviation from comparisons of 3 years and younger to older than 3 years (18+ normalization, no unit)

	Tract count	Volume	Length	FA	ADC
Anterior					
P values (under vs. over 3 YO)	**2.63×10^{-5}**	**5.34×10^{-7}**	**1.25×10^{-6}**	4.81×10^{-3}	6.67×10^{-3}
Under 3 YO: mean ± SD	0.52 ± 0.14	0.49 ± 0.12	0.69 ± 0.11	0.84 ± 0.18	1.07 ± 0.18
Over 3 YO: mean ± SD	0.83 ± 0.20	0.83 ± 0.18	0.88 ± 0.13	0.97 ± 0.09	1.01 ± 0.09
Middle					
P values (under vs. over 3 YO)	**3.93×10^{-9}**	**1.12×10^{-11}**	**1.05×10^{-7}**	7.92×10^{-1}	1.27×10^{-2}
Under 3 YO: mean ± SD	0.43 ± 0.11	0.41 ± 0.09	0.78 ± 0.08	0.96 ± 0.20	1.07 ± 0.21
Over 3 YO: mean ± SD	0.87 ± 0.22	0.88 ± 0.16	0.97 ± 0.08	1.00 ± 0.06	1.01 ± 0.10
Posterior					
P values (under vs. over 3 YO)	**9.71×10^{-9}**	**5.12×10^{-12}**	**1.14×10^{-8}**	2.53×10^{-3}	7.17×10^{-3}
Under 3 YO: mean ± SD	0.46 ± 0.20	0.46 ± 0.16	0.76 ± 0.13	0.83 ± 0.14	1.08 ± 0.21
Over 3 YO: mean ± SD	0.90 ± 0.23	0.91 ± 0.18	0.96 ± 0.10	0.96 ± 0.08	1.02 ± 0.09

*Statistically significant *P* values are bolded.

Table 3 *P* values, mean, and standard deviation from comparisons of 3 years and younger to older than 3 years (WB normalization, no unit)

	Tract count	Volume	Length	FA	ADC
Anterior					
P values (under vs. over 3 YO)	**7.23×10^{-6}**	**1.93×10^{-4}**	9.40×10^{-4}	**2.91×10^{-13}**	3.11×10^{-2}
Under 3 YO: mean ± SD	0.0016 ± 0.0006	0.0073 ± 0.0022	1.67 ± 0.22	1.12 ± 0.14	0.94 ± 0.07
Over 3 YO: mean ± SD	0.0011 ± 0.0003	0.0058 ± 0.0013	1.89 ± 0.24	1.37 ± 0.09	0.87 ± 0.05
Middle					
P values (under vs. over 3 YO)	2.94×10^{-2}	4.96×10^{-1}	3.41×10^{-2}	**6.73×10^{-6}**	5.91×10^{-3}
Under 3 YO: mean ± SD	0.0031 ± 0.0011	0.0126 ± 0.00312	3.04 ± 0.32	1.31 ± 0.15	0.92 ± 0.046
Over 3 YO: mean ± SD	0.0027 ± 0.0003	0.0127 ± 0.0015	3.34 ± 0.40	1.31 ± 0.19	0.98 ± 0.054
Posterior					
P values (under vs. over 3 YO)	1.00×10^{-1}	3.26×10^{-1}	**2.29×10^{-4}**	**1.99×10^{-10}**	2.75×10^{-3}
Under 3 YO: mean ± SD	0.0007 ± 0.0003	0.0046 ± 0.0015	3.45 ± 0.40	1.31 ± 0.19	0.98 ± 0.05
Over 3 YO: mean ± SD	0.0006 ± 0.0002	0.0044 ± 0.0008	3.92 ± 0.44	1.57 ± 0.11	0.91 ± 0.05

*Statistically significant *P* values are bolded.

Results also showed that regional differences in brain development in fetal ages persisted in postnatal development.

Multiple Neuronal Migration Pathways to the Thalamus

Through tractography, clearly distinct multiple pathways likely corresponding to neuronal migration pathways to the thalamus were detected in this study. One of such pathways from the anterior and posterior ventricular edges in ventral brain regions took a course just below the body of the GE: the main body of the GE showed strong coherency in the anterior–posterior direction as shown in our past tractography studies (Takahashi et al. 2012; Kolasinski et al. 2013; Miyazaki et al. 2016), while the pathways related to the thalamus were running oblique to the main GE pathways, reflecting the location of their destination, thalami. These results are well in agreement with past studies that showed the ventral telencephalon to be the place of origin of the cells that will eventually migrate to the thalamus (Rakić and Sidman 1969; Letinić and Kostović 1997; Corbin et al. 2001). We also successfully detected 3 pathways between the GE and the thalamus.

Vasung and colleagues reported that there were periventricular fiber (PVF) pathways taking a similar course as that of the GE. We admit that the pathways linked to the GE in this study might also include PVFs. However, the reported PVFs are significantly much thinner than the GE in this study, located along the edge of the GE, while we observed much thicker, strongly coherent pathways running through the GE.

Middle Segment of the TC Pathways—Migration Pathways? More Like Axons

While the anterior and posterior parts of the pathways related to the thalami clearly originated from the ventricular edge of the GE, the middle part of the pathways mostly went up into the deep regions in the cerebral mantle. During development, the TC axons go through a number of steps in order to reach their final positioning and are led through this path by neuroglial pathways (Rakić 1975, 1988). As their formation begins during early embryonic life, axonal pathways from the thalamus and cerebral cortex continue to grow separately to the GE, where they converge in hamsters (Métin and Godement 1996). Yet Molnár and colleagues (1998) provide evidence supporting the handshake hypothesis in rats, with thalamus and cortical fibers meeting within the internal capsule, before the TC pathways grow towards the cortex. Given the deep cerebral mantle regions where the middle part of the pathways related to the thalami terminate, pointing towards the cerebral cortex, it is likely that those pathways are not related to neuronal migration but rather emerging axonal pathways. Kostovic and Vasung (2009) summarized that TC afferent pathways are observed between 17 and 25 GW, which is well in agreement with our current results in the middle segment where

pathways likely related to axonal pathways were observed from 17 GW. In the other 2 segments, such pathways were detected only after 30 GW in this study, due to a sampling gap between 22 and 30 GW. Moreover, it is still unclear around when and how in the human brain neuronal migration to the middle part of the thalamus is completed. It is necessary to directly study earlier developmental stages in humans (e.g., from 11 GW in Wang et al. 2015) to conclude whether neurons in the middle part of the thalamus undergo secondary migration from either an anterior or a posterior thalamic region or directly migrate from the ventricular zone. Further investigations about regional variabilities of the period of neuronal migration will be necessary to understand regional variations of axonal emergence in fetal ages.

Neuronal Migration, Axonal Growth, and Pruning

In in vivo data, anterior TC pathways in the group of 3 years and younger had more WB-normalized tract number and volume than older than 3 years. Middle and posterior segments of the TC pathways did not show difference in WB-normalized tract number nor in volume before and after 3 years old. These results can be a parallel observation with our current ex vivo fetal results suggesting that a larger volume of anterior tractography pathways are likely linked to neuronal migration pathways to the thalamus. Our previous research also found that thinning of the radial migration pathway occurs from the posterior regions of the brain to anterior regions (Takahashi et al., 2012). One could speculate that extensive and/or protracted neuronal migration in the anterior part of the thalamus results in more neuronal and axonal fibers in the anterior TC pathways in early developmental ages.

Another possibility for the high number and volume of the anterior TC pathways is later pruning of neurons or axons in the anterior TC pathways compared with the middle and posterior TC pathways. TC axonal growth and pruning in rats over the first 3 weeks of postnatal life showed a balance between the 2, with axonal growth being favored during the first stages of development after birth (Portera-Cailliau et al. 2005): TC axons displayed a rapid rate of growth during these weeks compared with other cortical axons. Adult rats in another study (Oberlaender et al. 2012) showed a 25% decrease in overall TC arborization when exposed to a unique sensory experience, which in this study was the trimming of their whiskers, suggesting that sensory experiences can induce TC pruning. Many MRI studies have found a decrease in total thalamus volume as age increases (Xu et al. 2000; Van Der Werf et al. 2001; Sullivan et al. 2004). There has been evidence that the maturation of the human brain is continuous until adulthood (Giorgio et al. 2010; Peters et al. 2012; Chavarria et al. 2014; Li et al. 2014), and synaptic pruning has been suggested to occur until adolescence (Huttenlocher 1979; Giedd et al. 1999; Craik and Bialystok 2006). One study specifically found that dendritic spine density in childhood is between double to triple that of adults, and while it begins to decrease throughout adolescence, it is only completed after 30 years of age (Petanjek et al. 2011). Although the evidence for synaptic pruning in the literature is mostly from the decrease in gray matter volume, this may reflect the decrease in the tract count or volume of our tractography pathways because those include gray matter pathways with low FA values in our study as described in the "Materials and Methods" section.

In addition, interestingly, given that the pathways likely linked to thalamic neuronal migration and thalamocortical pathways were found to take the same course between the thalamus and either the ventricle or toward the cortex through the brain region (very close to the specific ventricle regions for the neuronal migration pathways), one could also speculate that axonal elongation from the thalamus occurs along neuronal migration pathways. The findings that the topography of the tractography pathways likely linked to neuronal migration pathways were in accordance with the known topography of the TC pathways also support this notion: there were tractography pathways between the anterior GE and medial thalamic regions while it is known that the TC pathways run between the anterior cerebral cortex and the medial thalamic nucleus (mediodorsal nucleus). There were also tractography pathways between middle-posterior GE to middle-posterior thalamus, while it is known that the TC pathways run between the middle-posterior cerebral cortices and middle-posterior thalamic nuclei (e.g., the ventral lateral nucleus, ventral posterolateral nucleus, and the pulvinar).

Regional Differences of Maturational Patterns

The tract count and volume in in vivo data showed differential regional variations: the middle segment had more tract count and volume than those of the anterior and the anterior segment had more tract count and volume than those of the posterior segment (posterior < anterior < middle). The results of the anterior and posterior segments are well in agreement with observations from postmortem fetal specimens in which between the ventricular zone and thalami, more tractography pathways were found in the anterior regions compared with posterior regions. Regarding the middle segment, since the middle part of the brain includes primary sensory and motor areas, having the most volumetric brain regions at least in the medio-lateral direction, it is not surprising that the middle TC segment is thicker in the medio-lateral direction along the primary sensory/motor areas than the other 2 TC segments. Even when the majority of the detected anterior and posterior tractography pathways seemed to be related to neuronal migratory pathways, the middle part of the detected tractography pathways seemed to be already related to emerging axonal pathways, one could speculate that the middle part of neuronal migration to the thalamus terminates earlier than the other parts, and the middle part of TC pathways becomes mature sooner than the other parts with continuously progressing myelination, which may contribute to the large volume of the middle segment. However, the potential early termination of neuronal migration to the middle part of the thalamus might result in fewer thalamic neurons in that part, which could conflict with more tract count and larger volume in the middle TC pathways observed in this study. Future studies will be necessary to describe detailed regional differences of neuronal migration and emergence of TC pathways.

It was previously found that FA increases with gestational age in the projections from the thalami, which suggest significant microscopic structural changes in these areas during development. Even in brain regions where myelin is not yet present, the FA increases, suggesting oligodendrocyte ensheathment (Aeby et al. 2009). Our data support this, and as the TC fibers become myelinated and mature throughout late prenatal and postnatal development, they tend to maintain the same path, but elongate and prune as necessary. This study focuses more on prenatal development as we found this time period was when the most significant developmental changes occur on a macroscopic level. Previously, studies have indicated

the importance of afferent fibers, particularly TC ones, in regulating the area-specific differentiation of the developing brain (O'Leary et al. 1994). Should these fibers develop incorrectly, it can lead to serious problems in cortical morphogenesis and other aspects of development may be interrupted. Previous research has found that in preterm infants higher-order cortical areas had reduced corticothalamic connections, especially in frontoparietal, prefrontal, and anterior cingulate cortex regions. These regions are crucial in task-based functioning in adults, and this could explain the higher rates of attention deficits, anxiety, and autism spectrum disorders that occur in those born prematurely (Toulmin et al. 2015).

The results of length comparisons that the middle segment is in average longer than the length of the anterior segment is expected from the results of tract count and volume. However, the posterior segment had the least tract count and volume, but the longest length with high FA values. These results together suggest that the posterior TC pathways are the most tightly packed, while the density of the pathways between the anterior and middle segments is proportional (anterior < middle). Given that some previous studies reported a higher neural density in the posterior than in the anterior brain region in primates (Cahalane et al. 2012; Charvet et al. 2015) in adults, it may be possible that a higher neuronal density in the posterior cerebral cortex contributes a higher density of posterior TC axons and tractography pathways, and the anterior–posterior gradient in the TC development.

Limitations of This Study and Future Directions

While DTI has come in useful in the past to study the GE, thalamus, and the development of other subcortical structures (Huang et al. 2009), HARDI is superior in analyzing crossing fibers, especially in unmyelinated brains. In this study, as other diffusion MRI studies, we assumed that pathways likely linked to neuronal migration and TC pathways were detected, based on the knowledge from the literature. Using diffusion MRI, we usually measure water diffusivity without directly measuring axonal pathways or neuronal migration pathways (Mori and van Zijl 2002; Frank 2002; Tournier et al. 2004; Takahashi et al. 2012). However, we admit that this limitation is part of the nature of current diffusion MRI studies and that histology is superior to MRI in terms of spatial resolution and directness. Although histology has a different type of limitation, which precludes the study of global fiber connections, future confirmation of our current results with histology will help understanding how well diffusion MRI tractography can reveal neuronal migration and emerging TC pathways. While we have found an interesting spatial topography between the thalamic regions and the GE that is well compatible with known topography of TC pathways, it would be beneficial to identify each thalamic nucleus in the human fetus and see more detailed spatial relationships of the pathways from each nucleus. Currently, it is difficult to 3-dimensionally evaluate the TC development in early fetal ages in vivo. Therefore, postmortem analyses on MR data would be an important first step toward this purpose in the age range studied in the current research as well as in even earlier ages (Kostovic and Vasung 2009; Wang et al. 2015).

Through MR imaging, it has been shown that preterm babies are affected by having less developed TC pathways, which is correlated with cognitive performance in early childhood (Ball et al. 2015). Disturbances to the development of the TC system can cause detrimental defects later in life, possibly leading to schizophrenia (Marenco et al. 2012; Klingner et al. 2014), autism (Nair et al. 2013), and bipolar disorder (Anticevic et al. 2014). TC projections are also involved in reading, as dyslexic individuals have been known to show hyperactivation of the TC system (Bruni et al. 2009). Future studies will challenge to characterize abnormal developmental time courses, potential aberrant trajectories, and other pathologies of the TC pathways (Wilkinson et al. 2016).

The TC pathways are known to play important roles in healthy sleep patterns: clear cyclical variations of electroencephalography activity corresponding to early sleep–wake cycles have been found in preterm infants as young as 27 GW, which have been hypothesized to represent switches between TC and corticocortical sleep pattern generators (Kuhle et al. 2001). Disturbed sleep pattern and schedule are observed in infants through adults with wide range of developmental and cognitive disorders (Cohrs 2008; Accardo and Malow 2014; Robillard et al. 2015). We believe that this study will be a useful reference for the normal TC development in future clinical imaging studies.

Supplementary Material

Supplementary material can be found at: http://www.cercor.oxfordjournals.org/.

Funding

This work was supported by NIH (R01HD078561, R21HD069001, R03NS091587) (ET). This research was carried out in part at the Athinoula A. Martinos Center for Biomedical Imaging at the Massachusetts General Hospital, using resources provided by the *Center for Functional Neuroimaging Technologies,* NIH *P41RR14075*, a P41 Regional Resource supported by the Biomedical Technology Program of the National Center for Research Resources (NCRR), National Institutes of Health. This work also involved the use of instrumentation supported by the NCRR Shared Instrumentation Grant Program (NIH S10RR023401, S10RR019307, and S10RR023043) and High-End Instrumentation Grant Program (NIH S10RR016811). This study was conducted partly using postmortem human brain specimens from the tissue collection at the Department of Neurobiology at Yale University School of Medicine (supported by grant NIH MH081896), which form a part of the BrainSpan Consortium collection (http://www.brainspan.org).

Notes

The other brain specimens were kindly provided by Dr. Rebecca D. Folkerth, Brigham and Women's Hospital, Boston Children's Hospital, and Harvard Medical School. *Conflict of Interest*: None declared.

References

Accardo JA, Malow BA. 2014. Sleep, epilepsy, and autism. Epilepsy Behav. Doi:10.1016/j.yebeh.2014.09.081.[Epub ahead of print].

Aeby A, Liu Y, De Tiège X, Denolin V, David P, Balériaux D, Kavec M, Metens T, Van Bogaert P. 2009. Maturation of thalamic radiations between 34 and 41 weeks gestation: a combined voxel-based study and probabilistic tractography with diffusion tensor imaging. Am J Neuroradiol. 30:1780–1786.

Alcauter S, Lin W, Smith JK, Short SJ, Goldman BD, Reznick JS, Gilmore JH, Gao W. 2014. Development of thalamocortical

connectivity during infancy and its cognitive correlations. J Neurosci. 34:9067–9075.
Anticevic A, Cole MW, Repovs G, Murray JD, Brumbaugh MS, Winkler AM, Savic A, Krystal JH, Pearlson GD, Glahn DC. 2014. Characterizing thalamo-cortical disturbances in schizophrenia and bipolar illness. Cereb Cortex. 24: 3116–3130.
Ball G, Pazderova L, Chew A, Tusor N, Merchant N, Arichi T, Allsop JM, Cowan FM, Edwards AD, Counsell SJ. 2015. Thalamocortical connectivity predicts cognition in children born preterm. Cereb Cortex. 25:4310–4318.
Bayer SA, Altman J. 2005. The Human Brain During the Second Trimester. Florida, USA: CRC Press.
Berchicci M, Zhang T, Romero L, Peters A, Annett R, Teuscher U, Bertollo M, Okada Y, Stephen J, Comani S. 2011. Development of mu rhythm in infants and preschool children. Dev Neurosci. 33:130–143.
Berthier NE, DeBlois S, Poirier CR, Novak MA, Clifton RK. 2000. Where's the ball? Two- and three-year-olds reason about unseen events. Dev Psychol. 36:394–401.
Bruni O, Ferri R, Novelli L, Finotti E, Terribili M, Troianiello M, Valente D, Sabatello U, Curatolo P. 2009. Slow EEG amplitude oscillations during NREM sleep and reading disabilities in children with dyslexia. Dev Neuropsychol. 34:539–551.
Bystron I, Blakemore C, Rakic P. 2008. Development of the human cerebral cortex: Boulder Committee revisited. Nat Rev Neurosci. 9 (2):110–122.
Cahalane DJ, Charvet CJ, Finlay BL. 2012. Systematic, balancing gradients in neuron density and number across the primate isocortex. Front Neuroanat. 6:28.
Catalano SM, Shatz CJ. 1998. Activity-dependent cortical target selection by thalamic axons. Science. 281:559–562.
Catani M, Thiebaut de Schotten M. 2008. A diffusion tensor imaging tractography atlas for virtual in vivo dissections. Cortex. 44:1105–1132.
Caviness VS, Kennedy DN, Bates J, Makris N. 1996. The developmental neuroimaging: Mapping the development of brain and behaviour. New York: Academic Press. p. 3–14.
Charvet CJ, Cahalane DJ, Finlay BL. 2015. Systematic, cross-cortex variation in neuron numbers in rodents and primates. Cereb Cortex. 25:147–160.
Chavarria MC, Sánchez FJ, Chou Y, Thompson PM, Luders E. 2014. Puberty in the corpus callosum. Neuroscience. 18:1–8.
Cohen AH, Wang R, Wilkinson M, MacDonald P, Lim AR, Takahashi E. 2016. Development of human white matter fiber pathways: from newborn to adult ages. Int J Dev Neurosci. 50:26–38.
Cohrs S. 2008. Sleep disturbances in patients with schizophrenia: impact and effect of antipsychotics. CNS Drugs. 22: 939–962.
Corbin JG, Nery S, Fishell G. 2001. Telencephalic cells take a tangent: non-radial migration in the mammalian forebrain. Nat Neurosci. 4:1177–1182.
Craik FIM, Bialystok E. 2006. Cognition through the lifespan: mechanisms of change. Trends Cogn Sci. 10:131–138.
Frank LR. 2002. Characterization of anisotropy in high angular resolution diffusion-weighted MRI. Magn Reson Med. 47: 1083–1099.
Frassoni C, Amadeo A, Ortino B, Jaranowska A, Spreafico R. 2000. Organization of radial and non-radial glia in the developing rat thalamus. J Comp Neurol. 428:527–542.
Galaburda AM. 2005. Dyslexia—a molecular disorder of neuronal migration. Ann Dyslexia. 55:151–165.
Giedd JN, Blumenthal J, Jeffries NO, Castellanos FX, Liu H, Zijdenbos A, Paus T, Evans AC, Rapaport JL. 1999. Brain development during childhood and adolescence: a longitudinal MRI study. Nat Neurosci. 2:861–863.
Giorgio A, Watkins KE, Chadwick M, James S, Winmill L, Douaud G, De Stefano N, Matthews PM, Smith SM, Johansen-Berg H, et al. 2010. Longitudinal changes in grey and white matter during adolescence. Neuroimage. 49: 94–103.
Gredebäck G, Kochukhova O. 2010. Goal anticipating during action observation is influenced by synonymous action capabilities, a puzzling development study. Exp Brain Res. 202: 493–497.
Hong JH, Son SM, Jang SH. 2010. Identification of spinothalamic tract and its related thalamocortical fibers in human brain. Neurosci Lett. 468:102–105.
Huang H, Xue R, Zhang J, Ren T, Richards LJ, Yarowsky P, Miller MI, Mori S. 2009. Anatomical characterization of human fetal brain development with diffusion tensor magnetic resonance imaging. J Neurosci. 29:4263–4273. doi:10.1523/jneurosci.2769-08.2009.
Huttenlocher PR. 1979. Synaptic density in human frontal cortex—developmental changes and effects of aging. Brain Res. 163:195–205.
Jaermann T, De Zanche N, Staempfli P, Pruessmann KP, Valavanis A, Boesiger P, Kollias SS. 2008. Preliminary experience with visualization of intracortical fibers by focused high-resolution diffusion tensor imaging. Am J Neuroradiol. 29:146–150.
Jang SH, Yeo SS. 2013. Thalamocortical tract between anterior thalamic nuclei and cingulate gyrus in the human brain: diffusion tensor tractography study. Brain Imaging Behav. 7: 236–241.
Johansen-Berg H, Behrens TEJ, Sillery E, Ciccarelli O, Thompson A, Smith SM, Matthews PM. 2005. Functional-anatomical validation and individual variation of diffusion tractography-based segmentation of the human thalamus. Cereb Cortex. 15:31–39.
Jones EG. 1997. Cortical development and thalamic pathology in schizophrenia. Schizophr Bull. 23:483–501.
Jones EG. 2007. The Thalamus. 2nd ed.. Cambridge (MA): Cambridge University.
Keen R, Shutts K. 2007. Object and event representation in toddlers. Prog Brain Res. 164:227–235.
Keitel A, Prinz W, Friederici AD, von Hofsten C, Daum MM. 2013. Perception of conversations: the importance of semantics and intonation in children's development. J Exp Child Psychol. 116:264–277.
Klein JC, Rushworth MFS, Behrens TEJ, Mackay CE, de Crespigny AJ, D'Arceuil H, Johansen-Berg H. 2010. Topography of connections between human prefrontal cortex and mediodorsal thalamus studied with diffusion tractography. Neuroimage. 51:555–564.
Klingner CM, Langbein K, Dietzek M, Smesny S, Witte OW, Sauer H, Nenadic I. 2014. Thalamocortical connectivity during resting state in schizophrenia. Eur Arch Psychiatry Clin Neurosci. 264:111–119.
Kostovic I, Rakic P. 1984. Development of prestriate visual projections in the monkey and human fetal cerebrum revealed by transient cholinesterase staining. J Neurosci. 4:25–42.
Kostovic I, Vasung L. 2009. Insights from in vitro fetal magnetic resonance imaging of cerebral development. Semin Perinatol. 33:220–233.

Kolasinski J, Takahashi E, Stevens AA, Benner T, Fischl B, Zöllei L, Grant PE. 2013. Radial and tangential neuronal migration pathways in the human fetal brain: anatomically distinct patterns of diffusion MRI coherence. Neuroimage. 79: 412–422.

Kuhle S, Klebermass K, Olischar M, Hulek M, Prusa AR, Kohlhauser C, Birnbacher R, Weninger M. 2001. Sleep-wake cycles in preterm infants below 30 weeks of gestational age. Preliminary results of a prospective amplitude integrated EEG study. Wien Klin Wochenschr. 113:219–223.

Letinić K, Kostović I. 1997. Transient fetal structure, the gangliothalamic body, connects telencephalic germinal zone with all thalamic regions in the developing human brain. J Comp Neurol. 384:373–395.

Letinić K, Rakić P. 2001. Telencephalic origin of human thalamic GABAergic neurons. Nat Neurosci. 4:931–936.

Li W, Wu B, Batrachenko A, Bancroft-Wu V, Morey RA, Shashi V, Langkammer C, De Bellis MD, Ropele S, Song AW, Liu C. 2014. Differential developmental trajectories of magnetic susceptibility in human brain gray and white matter over the lifespan. Hum Brain Mapp. 35:2698–2713.

Lippé S, Martinez-Montes E, Arcand C, Lassonde M. 2009. Electrophysiological study of auditory development. Neuroscience. 164:1108–1118.

Llinás R. 2003. Consciousness and the thalamocortical loop. Int Congr Ser. 1250:409–416.

Marenco S, Stein JL, Savostyanova AA, Sambataro F, Tan HY, Goldman AL, Verchinski BA, Barnett AS, Dickinson D, Apud JA, et al. 2012. Investigation of anatomical thalamo-cortical connectivity and fMRI activation in schizophrenia. Neuropsychopharmacology. 37:499–507.

McKinstry RC, Mathur A, Miller JH, Ozcan A, Snyder AZ, Schefft GL, Almli CR, Shiran SI, Conturo TE, Neil JJ. 2002. Radial organization of developing preterm human cerebral cortex revealed by non-invasive water diffusion anisotropy MRI. Cereb Cortex. 12:1237–1243.

Métin C, Godement P. 1996. The ganglionic eminence may be an intermediate target for corticofugal and thalamocortical axons. J Neurosci. 16:3219–3235.

Miyazaki Y, Song JW, Takahashi E. 2016. Asymmetry of radial and symmetry of tangential neuronal migration pathways in developing human fetal brains. Front Neuroanat. 10:2.

Molnár Z, Adams R, Blakemore C. 1998. Mechanisms underlying the early establishment of thalamocortical connections in the rat. J Neurosci. 18:5723–5745.

Molnár Z, Higashi S, López-Bendito G. 2003. Choreography of early thalamocortical development. Cereb Cortex. 13: 661–669.

Mori S, van Zijl PC. 2002. Fiber tracking: principles and strategies—a technical review. NMR Biomed. 15 (7–8):468–480.

Mori S, van Zijl P. 2007. Human white matter atlas. Am J Psychiatry. 164:1005.

Nair A, Treiber JM, Shukla DK, Shih P, Müller RA. 2013. Impaired thalamocortical connectivity in autism spectrum disorder: a study of functional and anatomical connectivity. Brain. 136: 1942–1955.

Oberlaender M, Ramirez A, Bruno RM. 2012. Sensory experience restructures thalamocortical axons during adulthood. Neuron. 74:648–655.

O'Leary DD, Schlaggar BL, Tuttle R. 1994. Specification of neocortical areas and thalamocortical connections. Annu Rev Neurosci. 17:419–439.

Ortino B, Inverardi F, Morante-Oria J, Fairén A, Frassoni C. 2003. Substrates and routes of migration of early generated neurons in the developing rat thalamus. Eur J Neurosci. 18: 323–332.

Petanjek Z, Berger B, Esclapez M. 2009a. Origins of cortical GABAergic neurons in the cynomolgus monkey. Cereb Cortex. 19 (2):249–262.

Petanjek Z, Kostović I, Esclapez M. 2009b. Primate-specific origins and migration of cortical GABAergic neurons. Front Neuroanat. 3:26.

Petanjek Z, Judas M, Simic G, Rasin MR, Uylings HBM, Rakic P, Kostovic I. 2011. Extraordinary neoteny of synaptic spines in the human prefrontal cortex. Proc Natl Acad Sci. 108: 13281–13286.

Peters BD, Szeszko PR, Radua J, Ikuta T, Gruner P, DeRosse P, Zhang JP, Giorgio A, Qiu D, Tapert SF, et al. 2012. White matter development in adolescence: diffusion tensor imaging and meta-analytic results. Schizophr Bull. 38:1308–1317.

Portera-Cailliau C, Weimer RM, De Paola V, Caroni P, Svoboda K. 2005. Diverse modes of axon elaboration in the developing neocortex. PLoS Biol. 3:e272.

Rakic P. 1972. Mode of cell migration to the superficial layers of fetal monkey neocortex. J Comp Neurol. 145 (1):61–83.

Rakic P. 1988. Specification of cerebral cortical areas. Science. 241 (4862):170–176.

Rakić P, Sidman RL. 1969. Telencephalic origin of pulvinar neurons in the fetal human brain. Z Anat Entwicklungsgesch. 129:53–82.

Rakić P. 1975. Timing of major ontogenetic events in the visual cortex of the monkey. In: Buckwald NA, Brazier M, editors. Brain Mechanisms in Mental Retardation. New York (NY): Academic Press. p. 3–40.

Rakić P. 1988. Defects of neuronal migration and the pathogenesis of cortical malformations. Prog Brain Res. 73:15–37.

Rao Y, Wu JY. 2001. Neuronal migration and the evolution of the human brain. Nat Neurosci. 4:860–862.

Robillard R, Hermens DF, Naismith SL, White D, Rogers NL, Ip TK, Mullin SJ, Alvares GA, Guastella AJ, Smith KL, et al. 2015. Ambulatory sleep-wake patterns and variability in young people with emerging mental disorders. J Psychiatry Neurosci. 40:28–37.

Sarnthein J, Morel A, von Stein A, Jeanmond D. 2005. Thalamocortical theta coherence in neurological patients at rest and during at working memory task. Int J Psychophysiol. 57:87–96.

Schimdt HJ, Beauchamp GK. 1988. Adult-like odor preferences and aversions in three-year-old children. Child Dev. 59: 1136–1143.

Schmahmann JD, Pandya DN, Wang R, Dai G, D'Arceuil HE, de Crespigny AJ, Wedeen VJ. 2007. Association fibre pathways of the brain: parallel observations from diffusion spectrum imaging and autoradiography. Brain. 130:630–653.

Seeley WW, Menon V, Schatzberg AF, Keller J, Glover GH, Kenna H, Reiss AL, Greicius MD. 2007. Dissociable intrinsic connectivity networks for salience processing and executive control. J Neurosci. 27:2349–2356.

Sidman RL, Rakić P. 1973. Neuronal migration, with special reference to developing human brain: a review. Brain Res. 62: 1–35.

Smith JP, Glass DJ, Fireman G. 2015. The understanding and experience of mixed motions in 3-5-year-old children. J Genet Psychol. 176:65–81.

Song JW, Mitchell PD, Kolasinski J, Ellen Grant P, Galaburda AM, Takahashi E. 2015. Asymmetry of White Matter Pathways in Developing Human Brains. Cereb Cortex. 25: 2883–2893.

Sullivan EV, Rosenbloom M, Serventi KL, Pfefferbaum A. 2004. Effects of age and sex on volumes of the thalamus, pons, and cortex. Neurobiol Aging. 25:185–192.

Takahashi E, Dai G, Rosen GD, Wang R, Ohki K, Folkerth RD, Galaburda AM, Wedeen VJ, Grant PE. 2011. Developing neocortex organization and connectivity in cats revealed by direct correlation of diffusion tractography and histology. Cereb Cortex. 21:200–211.

Takahashi E, Dai G, Wang R, Ohki K, Rosen GD, Galaburda AM, Grant PE, Wedeen VJ. 2010. Development of cerebral fiber pathways in cats revealed by diffusion spectrum imaging. Neuroimage. 49:1231–1240.

Takahashi E, Folkerth RD, Galaburda AL, Grant PE. 2012. Emerging cerebral connectivity in the human fetal brain: an MR tractography study. Cereb Cortex. 22:455–464.

Takahashi E, Hayahisi E, Schmahmann JD, Grant PE. 2014. Development of cerebellar connectivity in human fetal brains revealed by high angular resolution diffusion tractography. Neuroimage. 96:326–333.

Thiebaut de Schotten M, Ffytche DH, Bizzi A, Dell'Acqua F, Allin M, Walshe M, Murray R, Williams SC, Murphy DG, Catani M. 2011. Atlasing location, asymmetry and inter-subject variability of white matter tracts in the human brain with MR diffusion tractography. Neuroimage. 54:49–59.

Thompson RA. 2001. Development in the first years of life. Future Child. 11:20–33.

Toulmin H, Beckmann CF, O'Muircheartaigh J, Ball G, Nongena P, Makropoulos A, Ederies A, Counsell SJ, Kennea N, Arichi T, et al. 2015. Specialization and integration of functional thalamocortical connectivity in the human infant. Proc Natl Acad Sci USA. 112 (20):6485–6490.

Tournier JD, Calamante F, Gadian DG, Connelly A. 2004. Direct estimation of the fiber orientation density function from diffusion-weighted MRI data using spherical deconvolution. Neuroimage. 23:1176–1185.

Tournier JD, Calamante F, Connelly A. 2007. Robust determination of the fibre orientation distribution in diffusion MRI: non-negativity constrained super-resolved spherical deconvolution. Neuroimage. 35:1459–1472.

Tuch DS. 2004. Q-ball imaging. Magn Reson Med. 52:1358–1372.

Van Der Werf YD, Tisserand DJ, Visser PJ, Hofman PA, Vuurman E, Uylings HB, Jolles J. 2001. Thalamic volume predicts performance on tests of cognitive speed and decreases in healthy aging. A magnetic resonance imaging-based volumetric analysis. Cogn Brain Res. 11:377–385.

Wakana S, Jiang H, Nagae-Poetscher LM, van Zijl PC, Mori S. 2004. Fiber tract-based atlas of human white matter anatomy. Radiology. 230:77–87.

Wang R, Dai G, Takahashi E. 2015. High resolution MRI reveals detailed layer structures in early human fetal stages: in vitro study with histologic correlation. Front Neuroanat. 9:150.

Wedeen VJ, Wang RP, Schmahmann JD, Benner T, Tseng WY, Dai G, Pandya DN, Hagmann P, D'Arceuil H, de Crespigny AJ. 2008. Diffusion spectrum magnetic resonance imaging (DSI) tractography of crossing fibers. Neuroimage. 41:1267–1277.

Whiten A, Flynn E, Brown K, Lee T. 2006. Imitation of hierarchical action structure by young children. Dev Sci. 9:574–582.

Wilkinson M, Wang R, van der Kouwe A, Takahashi E. 2016. White and gray matter fiber pathways in autism spectrum disorder revealed by *ex vivo* diffusion MR tractography. Brain Behav. 6:e00483. doi: 10.1002/brb3.483.

Wonders CP, Anderson SA. 2006. The origin and specification of cortical interneurons. Nat Rev Neurosci. 7 (9):687–696.

Xu J, Kobayashi S, Yamaguchi S, Iijima K, Okada K, Yamashita K. 2000. Gender effects on age-related changes in brain structure. Am J Neuroradiol. 21:112–118.

Xu G, Takahashi E, Folkerth RD, Haynes RL, Volpe JJ, Grant E, Kinney HC. 2014. Radial coherence of diffusion tractography in the cerebral white matter of the human fetus: neuroanatomic insights. Cereb Cortex. 24:579–592.

Yamada K, Nagakane Y, Yoshikawa K, Kizu O, Ito O, Kubota T, Akazawa K, Oouchi H, Matsushima S, Nakagawa M, et al. 2007. Somatotopic organization of thalamocortical projection fibers as assessed with MR tractography. Radiology. 242: 840–845.

Zhang D, Snyder AZ, Shimony JS, Fox MD, Raichle ME. 2010. Noninvasive functional and structural connectivity mapping of the human thalamocortical system. Cereb Cortex. 20: 1187–1194.